OPEN

Citation: Oncogenesis (2014) **3**, e126; doi:10.1038/oncsis.2014.40

www.nature.com/oncsis

ORIGINAL ARTICLE

EBAG9 modulates host immune defense against tumor formation and metastasis by regulating cytotoxic activity of T lymphocytes

T Miyazaki[1], K Ikeda[1], K Horie-Inoue[1], T Kondo[2], S Takahashi[3] and S Inoue[1,4,5]

Estrogen receptor-binding fragment-associated antigen 9 (*EBAG9*) is a primary estrogen-responsive gene that we previously identified in MCF-7 breast cancer cells using the CpG genomic binding-site cloning technique. The expression of EBAG9 protein is often upregulated in malignant tumors, suggesting that this protein is involved in cancer pathophysiology. In the present study, we investigated the role of EBAG9 in host defense against implanted tumors in *Ebag9*-knockout (*Ebag9*KO) mice. MB-49 mouse bladder cancer cells were subcutaneously implanted into *Ebag9*KO and control mice. We found that tumor formation and metastasis to the lung by MB-49 cells were substantially reduced in *Ebag9*KO mice compared with control mice. The infiltration of $CD8^+$, $CD3^+$ and $CD4^+$ T cells into the generated tumors was enhanced in *Ebag9*KO mice compared with controls. Notably, $CD8^+$ T cells isolated from tumors in *Ebag9*KO mice exhibited substantial upregulation of immunity- and chemoattraction-related genes, including interleukin-10 receptor, interferon gamma, granzyme A, granzyme B and chemokine (C-X-C motif) receptor 3 compared with $CD8^+$ T cells from tumors in control mice. The $CD8^+$ T cells isolated from tumors in *Ebag9*KO mice also exhibited enhanced degranulation and increased cytolytic activity. Furthermore, the adoptive transfer of $CD8^+$ T cells isolated from tumors in *Ebag9*KO host could repress tumor growth by MB-49 cells implanted in wild-type host. These results suggest that EBAG9 modulates tumor growth and metastasis by negatively regulating the adaptive immune response in host defense. EBAG9 could be a potential target for tumor immunotherapy.

Oncogenesis (2014) **3,** e126; doi:10.1038/oncsis.2014.40; published online 3 November 2014

INTRODUCTION

Estrogen receptor-binding fragment-associated antigen 9 (*EBAG9*) is an estrogen-responsive gene that was originally isolated from a CpG island library of MCF-7 human breast cancer cells using a genomic binding-site cloning method.[1] EBAG9 is expressed in estrogen target organs as well as several other organs including the brain, liver, heart and kidney.[2] EBAG9 expression can be induced by estrogen, as observed in cell lines and in ovariectomized mice treated with 17β-estradiol. Although the physiological function of EBAG9 has not been well defined, the molecule may be implicated in cancer pathophysiology based on protein expression studies in breast,[3] ovarian,[4] prostate,[5] hepatocellular,[6] renal cell[7] and bladder cancers.[8] Furthermore, it has been shown that the immunoreactivity of EBAG9 positively correlates to advanced tumor grades and poor prognosis.[3–9] Therefore, EBAG9 is assumed to promote the progression of malignant tumors.

It has been reported that EBAG9 is localized in the Golgi apparatus and increases *O*-linked glycan expression.[10] The *O*-linked glycans, sialyl-Tn, is a carbohydrate antigen over-expressed in several epithelial cancers.[11] It has been shown that sialyl-Tn expression and concomitant changes in the overall *O*-glycan profile lead to a decreased adhesion and increased migration of MDA-MB-231 breast cancer cells. sialyl-Tn-positive MDA-MB-231 clones exhibit increased tumor growth in severe combined immunodeficiency mice.[11]

We have previously shown that EBAG9 has no significant effect on proliferation of Renca cells *in vitro*, whereas EBAG9 over-expression in Renca cells promotes tumor formation *in vivo* when the cells are implanted in BALB/c mice. Interestingly, in immunodeficient BALB/c nude mice, tumors generated by EBAG9-overexpressing Renca cells and vector-expressing Renca cells had similar volumes. Thus, EBAG9 is assumed to be a tumor-promoting factor rather than an essential oncoprotein by itself. The difference between EBAG9-overexpressing and vector-expressing Renca cells in terms of tumor growth in BALB/c mice could be owing to reduced numbers of infiltrating $CD8^+$ T cells in EBAG9-overexpressing Renca cell tumors, as a result of suppression of antitumor immunity in the micrenvironments.[7]

Cytotoxic T lymphocytes exclude tumor cells by releasing secretory lysosomes, which contain granzymes and perforin. These lysosomes are produced in the endoplasmic reticulum and subsequently transported to the Golgi complex.[12] It has been shown that the absence of EBAG9 enhances the cytotoxic activity of $CD8^+$ T cells in EBAG9-knockout mice. Although the absence of EBAG9 did not affectlymphocyte development, it led to an increased secretion of granzyme A from cytotoxic T lymphocytes

[1]Division of Gene Regulation and Signal Transduction, Research Center for Genomic Medicine, Saitama Medical University, Saitama, Japan; [2]KAST, Project on Health and Anti-aging, Kanagawa, Japan; [3]Department of Anatomy and Embryology, Graduate School of Comprehensive Human Sciences, University of Tsukuba, Tsukuba, Japan; [4]Department of Geriatric Medicine, Graduate School of Medicine, The University of Tokyo, Tokyo, Japan and [5]Department of Anti-Aging Medicine, Graduate School of Medicine, The University of Tokyo, Tokyo, Japan. Correspondence: Professor S Inoue, Department of Geriatric Medicine, Graduate School of Medicine, The University of Tokyo, 7-3-1 Hongo, Bunkyo-ku, Tokyo 113-8655, Japan.
E-mail: INOUE-GER@h.u-tokyo.ac.jp
Received 18 August 2014; revised 22 September 2014; accepted 30 September 2014

treated with CD3 antibody. EBAG9 is considered to inhibit endosomal-lysosomal trafficking of cytotoxic effectors.[13]

To assess the functional relevance of EBAG9 in host defense against tumors, we generated *Ebag9*-knockout (*Ebag9*KO) mice by crossing *Ebag9*$^{f/f}$ mice with *Ayu1-Cre* mice, which ubiquitously express Cre recombinase.[14] We show that *Ebag9*KO mice exhibit strong antitumor immune responses including tumor suppression of lung metastasis. Notably, in *Ebag9*KO mice, CD8$^+$ T-cell infiltration is significantly increased in generated tumors. We show that CD8$^+$ T cells in *Ebag9*KO mice exhibit increased expression of interleukin-10 receptor (*Il10r*), interferon gamma (*Ifng*), granzyme A (*Gzma*), granzyme B (*Gzmb*) and chemokine (C-X-C motif) receptor 3 (*Cxcr3*), as well as increased degranulation and cytotoxic activity. Moreover, adoptively transferred CD8$^+$ T cells isolated from tumors generated in *Ebag9*KO mice suppress tumor growth in wild-type mice.

RESULTS

Generation of *Ebag9*KO mice

To assess the physiological function of EBAG9 in host defense against tumors, we generated *Ebag9*KO mice by the following steps. We first generated *Ebag9*$^{f/f}$ mice by homologous recombination in embryonic stem cells (Figure 1a). Then, *Ebag9*$^{f/f}$ mice were crossed with *Ayu1-Cre* mice, which ubiquitously expressed Cre recombinase,[14] to remove the neomycin-resistance cassette and exon 2 of the *Ebag9* gene. The resulting heterozygous *Ebag9*$^{f/+}$; *Ayu1-Cre* mice were interbred to generate homozygous *Ebag9*$^{f/f}$; *Ayu1-Cre* (*Ebag9*KO) mice. Genotypes of progeny were confirmed by PCR using genomic DNA prepared from tails (Figure 1b). To confirm the absence of full-length *Ebag9* mRNA and protein expression in *Ebag9*KO mice, we examined *Ebag9* expression in mouse embryonic fibroblasts (MEFs) using quantitative real-time PCR (qRT–PCR) (Figure 1c) and western blot analysis (Figure 1d). Furthermore, we confirmed whether full-length *Ebag9* mRNA was deleted in brain, liver, spleen, bone marrow and thymus in *Ebag9*KO and control *Ebag9*$^{+/+}$;*Ayu1-Cre* mice using qRT–PCR (Figure 1e). The expression of full-length *Ebag9* mRNA and protein was completely abolished in *Ebag9*KO MEFs and tissues (including brain, liver, spleen, bone marrow and thymus). *Ebag9*KO mice seemed to be healthy and fertile without any apparent morphological abnormalities. In addition, mating of *Ebag9*KO mice produced normal litters.

Loss of Ebag9 in host suppresses tumor growth and lung metastasis by MB-49 bladder cancer cells

We investigated the role of EBAG9 in host tumor immunity using *Ebag9*KO mice with implanted tumors. MB-49 bladder cancer cells, which originated from a carcinogen-induced tumor of bladder epithelial origin in male C57BL/6 mice,[15] were inoculated into *Ebag9*KO and control mice. MB-49 cells developed smaller tumors in *Ebag9*KO mice than in control mice 4 weeks after inoculation (Figures 2a and b). After 4 weeks, the volume of tumors was significantly smaller in *Ebag9*KO mice than in control mice (2733 ± 1216 versus 5218 ± 1895 mm^3, $n = 8$, $P < 0.01$) (Figure 2c). Furthermore, to determine whether loss of EBAG9 is also involved in tumor metastasis, we investigated lung tissue in *Ebag9*KO and control mice. Tumor metastasis to the lung was significantly reduced in *Ebag9*KO mice compared with control mice (Figures 3a and b). After 4 weeks, the number of metastatic foci in the lung was significantly lower in *Ebag9*KO mice than in control mice (2.63 ± 2.39 versus 10.50 ± 3.39; *Ebag9*KO mice, $n = 8$; control mice, $n = 6$; $P < 0.01$) (Figure 3c). These results indicate that EBAG9 is involved in tumor growth and metastasis *in vivo*.

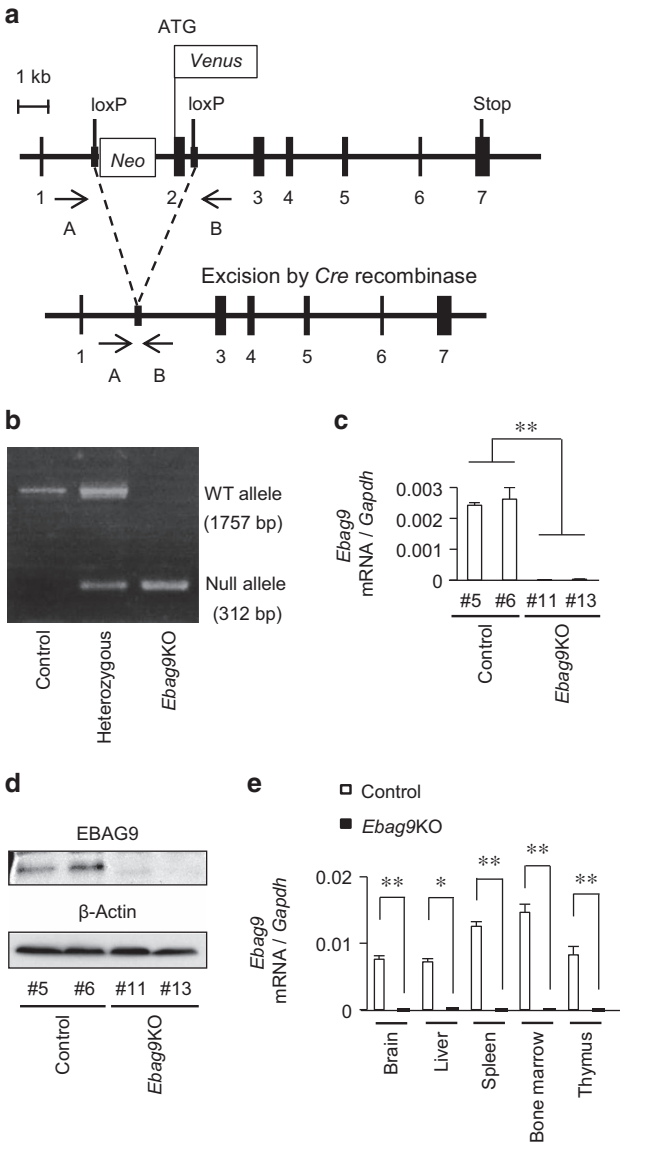

Figure 1. Generation of *Ebag9*KO mice. (**a**) Schematic representation of the strategy employed to disrupt the *Ebag9* gene. *Ebag9*$^{f/f}$ mice possess alleles including *loxP* sites flanking the neomycin-resistance cassette and *Ebag9* exon 2 (top). *Ebag9*$^{f/f}$ mice were crossed with *Ayu1-Cre* mice. After removal of the *loxP*-flanked neomycin-resistance cassette via Cre-mediated recombination (bottom), the resulting offspring has a heterozygous deletion of *Ebag9* (that is, *Ebag9*$^{f/+}$;*Ayu1-Cre*). *Ebag9*$^{f/+}$;*Ayu1-Cre* mice were bred to generate homozygous *Ebag9*$^{f/f}$;*Ayu1-Cre* mice, designated as *Ebag9*KO mice. Positions of the PCR primers A and B, used for genotyping, are shown. (**b**) Representative PCR analysis of genomic DNA from mouse tails. Genotyping was performed by PCR using primers A and B for the wild-type allele and the null allele. The genotypes and their corresponding PCR products are as follows: control (*Ebag9*$^{+/+}$;*Ayu1-Cre*), 1757 bp; heterozygous (*Ebag9*$^{f/+}$;*Ayu1-Cre*), 1757 and 312 bp; *Ebag9*KO (*Ebag9*$^{f/f}$;*Ayu1-Cre*), 312 bp. (**c**) qRT–PCR analysis of full-length *Ebag9* mRNA expression in MEFs obtained from *Ebag9*KO and control mice. *Gapdh* was used as an internal control. (**d**) Western blot analysis of EBAG9 protein expression in MEFs obtained from *Ebag9*KO and control mice. β-Actin was used as a loading control. (**e**) *Ebag9* mRNA expression in several tissues derived from *Ebag9*KO and control mice. *Ebag9* mRNA expression was analyzed by qRT–PCR. *Gapdh* was used as an internal control. The results shown are mean values ± s.d. $^*P < 0.05$; $^{**}P < 0.01$ by Student's *t*-test.

Increased infiltration of $CD8^+$, $CD3^+$, and $CD4^+$ T cells in implanted tumors of Ebag9KO mice

To explore whether EBAG9 modulates the subtype-specific reactivity of T cells against tumors, we examined the number of tumor-infiltrating T cells in the tumors generated in *Ebag9*KO and control mice by immunohistochemistry using antibodies specific for CD8, CD3, and CD4. Significant increases in the number of $CD8^+$ T cells (56.17 ± 22.05 versus 10.33 ± 11.07; *Ebag9*KO mice, $n = 8$; control mice, $n = 6$; $P < 0.01$) (Figure 4a), $CD3^+$ T cells (225.40 ± 39.06 versus 177.92 ± 31.87; *Ebag9*KO mice, $n = 8$; control mice, $n = 6$; $P < 0.01$) (Figure 4b), and $CD4^+$ T cells (62.32 ± 27.83 versus 42.91 ± 21.06; *Ebag9*KO mice, $n = 8$; control mice, $n = 6$; $P < 0.05$) (Figure 4c) in implanted tumors were observed in *Ebag9*KO mice.

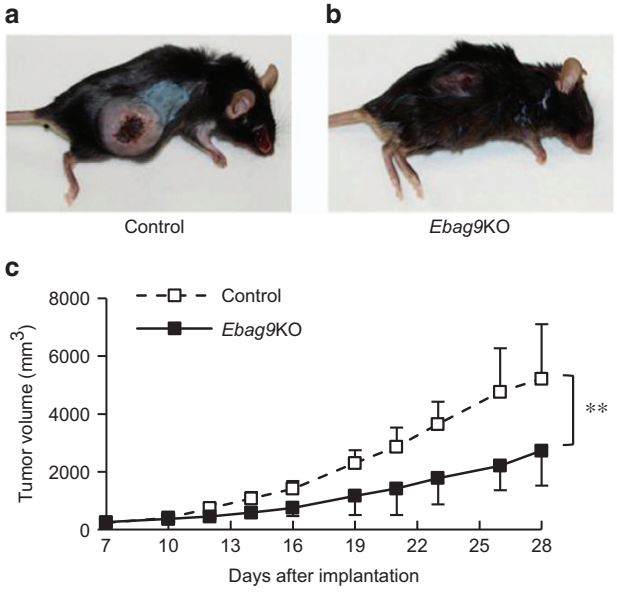

Figure 2. Reduced tumor growth of MB-49 bladder cancer cells implanted in *Ebag9*KO mice. MB-49 cells (5×10^5 cells per mouse) suspended in 50 µl of PBS were injected with 50 µl of Matrigel into the right flanks of *Ebag9*KO and control mice. Mice were sacrificed 28 days after implantation and tumors were excised. Representative photographs of control (**a**) and *Ebag9*KO mice (**b**) 4 weeks after inoculation with tumor cells. (**c**) Tumor volume in *Ebag9*KO mice is significantly smaller than that in control mice ($n = 8$ each). The data shown are mean values ± s.d. $^{**}P < 0.01$ by Student's *t*-test.

Upregulation of expression of immunity- and chemoattraction-related genes in $CD8^+$ T cells isolated from tumors generated in Ebag9KO mice

To investigate the role of EBAG9 in $CD8^+$ T-cell-mediated immune surveillance, we examined the expression of immunity- and chemoattraction-related genes in $CD8^+$ T cells isolated from tumors generated in *Ebag9*KO and control mice. The expression of *Il10r* (Figure 5a), *Ifng* (Figure 5b), *Gzma* (Figure 5c), *Gzmb* (Figure 5d) and *Cxcr3* (Figure 5e) was upregulated in $CD8^+$ T cells isolated from tumors generated in *Ebag9*KO mice compared with control mice (each $n = 3$, $P < 0.05$). We also confirmed that there was no detectable expression of full-length *Ebag9* mRNA (Figure 5f) in the $CD8^+$ T cells isolated from tumors generated in *Ebag9*KO mice by qRT–PCR ($n = 3$, $P < 0.01$). To measure the purity of $CD8^+$ T cells isolated from tumors generated in *Ebag9*KO and control mice, we stained the isolated cells with anti-CD8a-FITC antibody and analyzed the cells by flow cytometry. $CD8^+$ T cells typically constituted $>90\%$ of the isolated cells (data not shown). These results indicate that loss of EBAG9 resulted in the upregulation of genes related to cytotoxicity and chemoattraction.

Loss of EBAG9 induces host immune surveillance

We next performed a degranulation assay (Figure 6a) and a cytotoxicity assay (Figure 6b) to investigate whether the loss of EBAG9 expression influenced the activity of $CD8^+$ T cells. $CD8^+$ T cells isolated from tumors generated in *Ebag9*KO mice exhibited increased degranulation and cytotoxicity, suggesting that the loss of EBAG9 contributes to the fusion of lysosomes with the plasma membrane in $CD8^+$ T cells. Furthermore, we investigated whether the $CD8^+$ T cells isolated from tumors generated in *Ebag9*KO mice are involved in the suppression of bladder cancer MB-49 tumor growth. We intravenously transferred $CD8^+$ T cells isolated from tumors generated in *Ebag9*KO or control mice into C57BL/6 mice. Then, MB-49 cells were inoculated into the recipient mice. Adaptively transferred $CD8^+$ T cells isolated from tumors generated in *Ebag9*KO mice suppressed tumor growth of MB-49 cells (Figures 6c and d). After 13 days, adaptive transfer of $CD8^+$ T cells from *Ebag9*KO mice significantly inhibited tumor growth in C57BL/6 mice compared with those from control mice (333.9 ± 183.3 versus $616.5 \pm 107.3\ mm^3$, *Ebag9*KO mice, $n = 5$; control mice, $n = 7$; $P < 0.01$) (Figure 6e).

DISCUSSION

In the present study, we demonstrated that tumor formation and lung metastasis by implanted MB-49 mouse bladder cancer cells were substantially reduced in *Ebag9*KO mice compared with

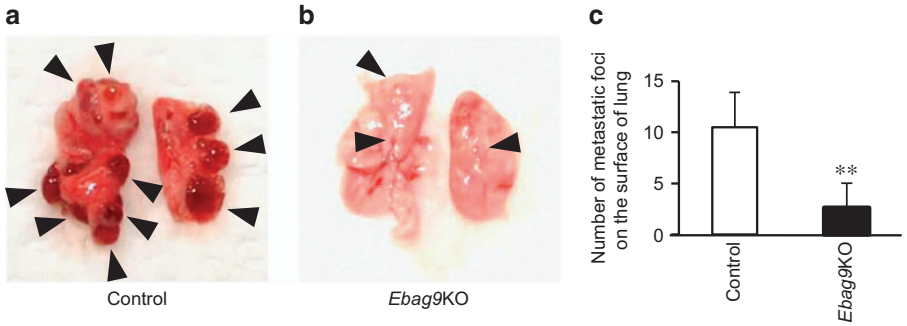

Figure 3. Reduced numbers of lung metastatic foci of MB-49 bladder cancer cells in *Ebag9*KO mice. Shown are representative photographs of control (**a**) and *Ebag9*KO mice (**b**) 4 weeks after inoculation with tumor cells. (**c**) Corresponding numbers of lung metastatic foci (control mice, $n = 6$; *Ebag9*KO mice, $n = 8$). The data shown are mean values ± s.d. $^{**}P < 0.01$ by Student's *t*-test.

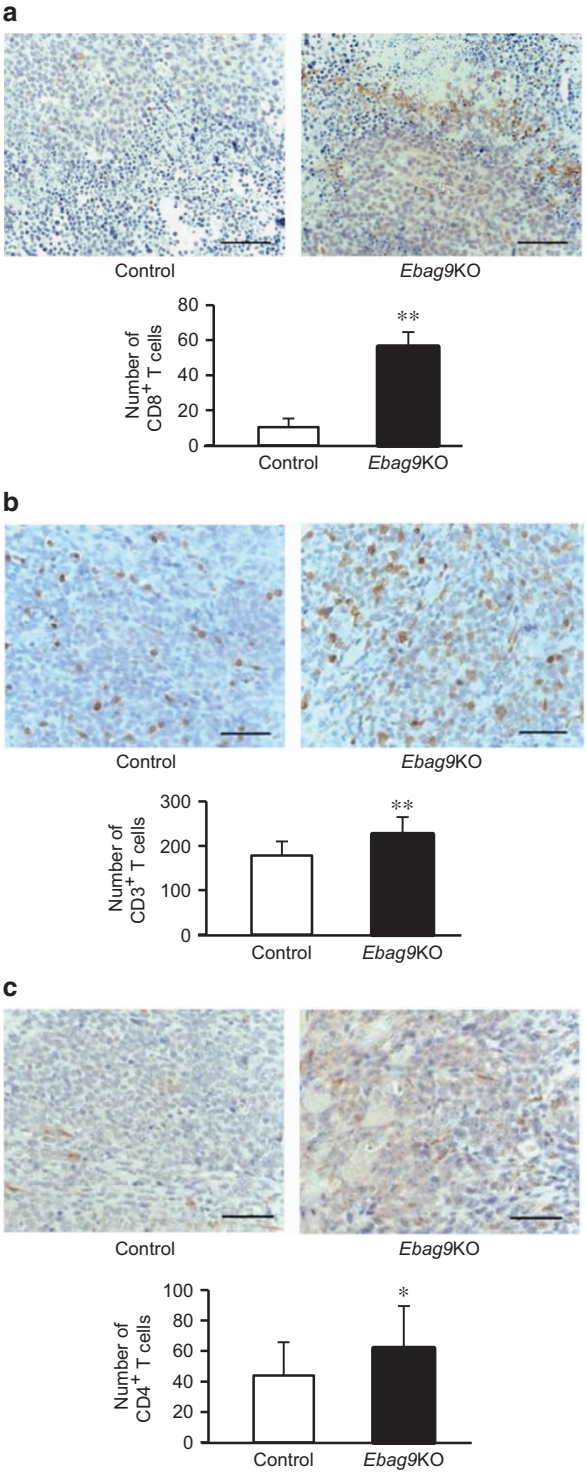

Figure 4. Increased numbers of $CD8^+$, $CD3^+$ and $CD4^+$ T cells in tumors generated in *Ebag9*KO mice. Paraffin sections of tumors generated in *Ebag9*KO and control mice were blocked in 0.3% $_{H2O2}$ and incubated with specific antibodies for CD8 (**a**), CD3 (**b**) or CD4 (**c**). Sections were then incubated with antirabbit EnVision+ reagent and counterstained with hematoxylin. Tumor-infiltrating lymphocytes positive for CD8 (**a**), CD3 (**b**) or CD4 (**c**) expression were microscopically counted in a high-power field of view at a magnification of 400× (*Ebag9*KO, $n=8$; control, $n=6$). The data shown in lower panels are mean values ± s.d. $^*P<0.05$; $^{**}P<0.01$ by Student's *t*-test. Scale bar, 20 μm.

control mice. Notably, in *Ebag9*KO mice, the numbers of infiltrating $CD8^+$, $CD3^+$ and $CD4^+$ T cells were significantly increased in tumors derived from MB-49 cells, and the expression of immunity- and chemoattraction-related genes was upregulated in $CD8^+$ T cells isolated from these tumors. EBAG9 was also found to be involved in the regulation of lysosome-mediated degranulation and cytotoxic activity of $CD8^+$ T cells. Furthermore, the adoptive transfer of $CD8^+$ T cells isolated from tumors in *Ebag9*KO host could repress tumor growth by MB-49 cells implanted in wild-type host. These results suggest that EBAG9 acts as a negative regulator of $CD8^+$ T cells in host immune surveillance against tumors.

In antitumor immunity, T-cell-mediated immune surveillance is a main host defense mechanism.[16] In this context, IL-10 is assumed to be an immunosuppressive cytokine within the tumor microenvironment. Recent studies have revealed, however, that IL-10 has rather diverse functions, as the molecule also induces potent antitumor responses.[17–19] It has been shown that IL-10 induces the proliferation and cytotoxic activity of $CD8^+$ T cells and functions as a chemoattractant for $CD8^+$ T cells.[20–23] Here we have shown that the loss of EBAG9 enhances antitumor responses in $CD8^+$ T cells, as these cells exhibited higher expression of *Il10r* in *Ebag9*KO mice than in controls. IL-10 activates $CD8^+$ T cells *in vitro*, and treatment with IL-10 leads to tumor rejection in multiple tumor-bearing mouse models.[24,25] IL-10 also increases the expression of IL-10R in activated $CD8^+$ T cells.[26] Furthermore, IL-10 treatment induces expression of interferon γ (IFN-γ) by $CD8^+$ T cells, which in turn increases levels of chemokines, such as CXCL9 (monokine induced by interferon, or MIG) and CXCL10 (interferon-induced protein of 10 kDa, or IP-10), in the tumor and serum.[27] These chemokines act as chemoattractants for T cells, suggesting a positive feedback loop of IFN-γ-producing $CD8^+$ T-cell recruitment into the tumor, initiated by IL-10. Indeed, such a feedback loop was proposed for mice bearing mammary tumors and treated with IL-10.[28] Overall, these results suggest that EBAG9 in $CD8^+$ T cells may act as a negative regulator of antitumor responses and that loss of EBAG9 function results in the activation of IL-10/IL-10R signaling.

CXCR3 is an inflammatory chemokine receptor present on activated T cells, particularly $CD4^+$ T cells and $CD8^+$ T cells.[29,30] CXCR3 has an important role in T-cell trafficking and function. Chemokines such as CXCL9, CXCL10 and CXCL11 function as CXCR3 ligands that induce cell migration.[29–32] It has been reported that these chemokines are abundantly expressed in CXCR3-positive cells involved in human and mouse cancers.[33–37] We have shown here that the expression of *Ifng* and *Cxcr3* is upregulated in *Ebag9*-deficient $CD8^+$ T cells. Our findings suggest that EBAG9 could be a negative regulator of cytotoxic activity and chemoattraction of T cells, resulting in the suppression of tumor immunosurveillance.

Degranulation of mature antigen-specific $CD8^+$ T cells is a requisite process for perforin- and granzyme-mediated killing of target cells.[38] We found that the loss of EBAG9 increased the expression of a degranulation marker, CD107, in $CD8^+$ T cells that had infiltrated tumors. This suggests that EBAG9 is involved in the regulation of endosomal trafficking of lytic granules in tumor-infiltrating T cells. Our findings are consistent with a previous report that EBAG9 deficiency increased the release of lytic granule contents and enhanced cytolytic capacity.[13]

We assume that the enhanced degranulation activity of $CD8^+$ T cells will primarily contribute to the magnitude of tumor inhibitory effects of *Ebag9*KO host in this study. We also consider that $CD8^+$ T cells with increased degranulation activity will secrete more amounts of cytokines and chemokines, such as IL-10, which lead to further chemoattraction of $CD8^+$ T cells and other immune-related cells into the tumors.[20–23] The number of infiltrating effector cells can be another major important factor for the magnitude of antitumor immunity, if the secretion of lytic

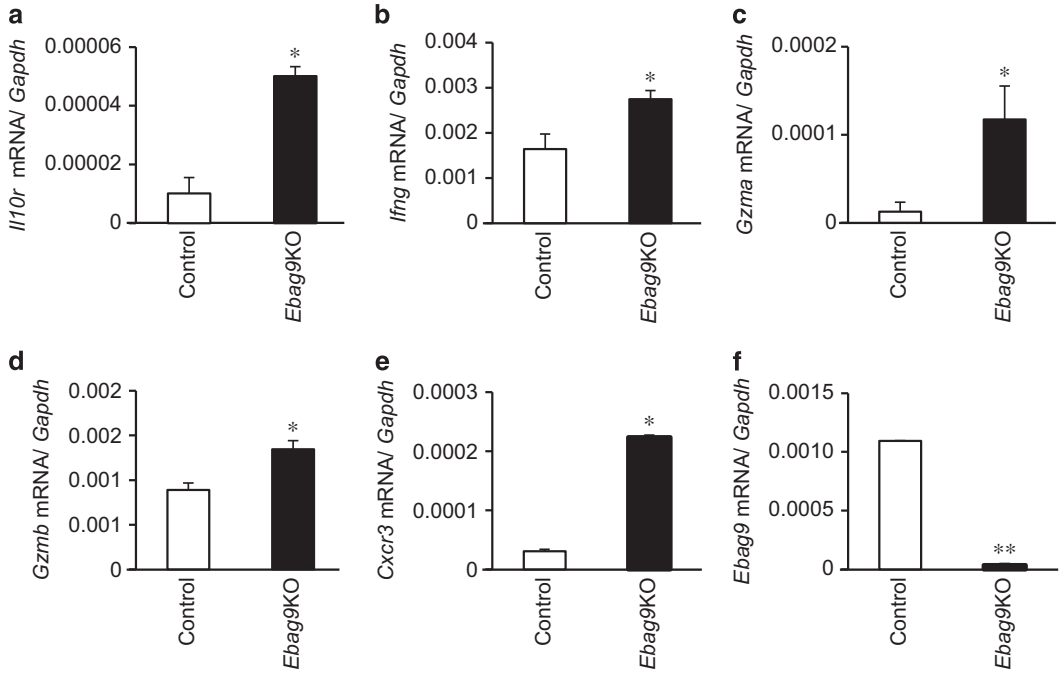

Figure 5. Upregulation of immunity- and chemoattraction-related genes in CD8$^+$ T cells isolated from tumors generated in *Ebag9*KO mice. mRNA levels of *Il10r* (**a**), *Ifng* (**b**), *Gzma* (**c**), *Gzmb* (**d**), *Cxcr3* (**e**) and *Ebag9* (**f**) were determined by qRT–PCR using RNAs prepared from CD8$^+$ T cells in tumors. The data shown are mean values ± s.d. $^*P < 0.05$, $^{**}P < 0.01$ by Student's *t*-test.

granules from CD8$^+$ T cells is stable and the cell frequency is a unique factor for the total amount of cytolytic activity.

In summary, our results show that EBAG9 is a critical factor that regulates T-cell-mediated antitumor immunity *in vivo*. Given these results and our previous findings regarding EBAG9 overexpression in cancers, we conclude that EBAG9 contributes to the promotion of tumor proliferation and the reduction of tumor immune surveillance. The management of EBAG9 expression in both tumors and their microenvironment could be an alternative therapeutic option for advanced stages of cancers.

MATERIALS AND METHODS

Reagents

Human anti-EBAG9 monoclonal antibody was generated against a glutathione *S*-transferase–EBAG9 fusion protein.[9] Antibodies against CD3 (Dako, Tokyo, Japan), CD4 (H-370; Santa Cruz Biotechnology, Dallas, DX, USA), CD8a (H-160; Santa Cruz Biotechnology), CD107-PE (1D4B; BD Pharmingen, Tokyo, Japan), CD8a–FITC (53-6.7; BD Pharmingen) and anti-β-actin (AC-74; Sigma-Aldrich, Tokyo, Japan) were purchased.

Bladdercancer cells

MB-49 mouse bladder cancer cells, which originated from a carcinogen-induced tumor of bladder epithelial origin in male C57BL/6 mice,[15] were maintained in RPMI 1640 containing 10% fetal calf serum, penicillin (50 U/ml) and streptomycin (50 mg/ml).

Generation of Ebag9KO mice

To generate *Ebag9* floxed (*Ebag9$^{f/f}$*) mice, genomic DNA covering the *Ebag9* locus was obtained from a 129SV/J mouse genomic library (Agilent Technologies, Santa Clara, CA, USA) by screening with a mouse *Ebag9* cDNA probe. The resulting DNA fragments were assembled into a targeting vector in which the *Venus* gene was inserted in frame at the translation initiation codon of the *Ebag9* gene and exon 2 was floxed by *loxP* sites (Figure 1a). After linearization, the targeting vector was electroporated into E14 embryonic stem cells.[39,40] G418-resistant colonies were selected and analyzed for homologous recombination by PCR and Southern blot hybridization. The primers for the PCR screening were 5′-GAGCACAAGGACAGATTGACCACGTCATGCAGGA-3′ and 5′-GTTGTGCCC AGTCATAGCCGAATAGCCTCTCCAC-3′. Positive clones were verified by Southern blot hybridization in which genomic DNA digested with PvuII was probed with a 414-bp DNA fragment corresponding to the 5′ upstream region of the *Ebag9* gene. The correctly targeted embryonic stem cells were injected into C57BL/6 blastocysts and transferred into pseudopregnant females. Chimeric offspring were bred to C57BL/6 mice expressing the Cre recombinase gene under the control of the ubiquitous *Ayu1* promoter (*Ayu1-Cre*).[14] Genotypes were determined by PCR analysis of tail DNA (Figure 1b). For amplification of the wild-type allele, the sense and antisense primers A (5′-GGGAAATTACTGTTGCTGGC-3′) and B (5′-CAGCTGAAGTATGTGTGCC-3′) were used (Figure 1a). For genotyping of *Ayu1-Cre* mice, primers derived from *Cre* (5′-CCTGGAAAATGCTTCTG TCCGTTTGCC-3′ and 5′-GAGTTGATAGCTGGCTGGTGGCAGATG-3′) were used to amplify a 653-bp product. Mice were kept under specific pathogen-free conditions and fed dry food and water *ad libitum*. All experiments were performed according to the guidelines for the care and use of laboratory animals of both the University of Tsukuba and Saitama Medical University.

Quantitative real-time PCR

Total RNAs were extracted from MEFs, brain, liver, spleen, bone marrow, thymus and CD8$^+$ T cells of *Ebag9*KO and control mice using ISOGEN reagent (Nippon Gene, Tokyo, Japan), and first-stand cDNA was generated with 1 μg of total RNA using SuperScript III reverse transcriptase (Invitrogen, San Diego, CA, USA) and oligo(dT)$_{20}$ primer. To evaluate the expression of mouse *Ebag9*, *Cd8*, *Il10r*, *Ifng*, *Gzma*, *Gzmb* and *Cxcr3* mRNA, RT-PCR was done using primers specific for mouse *Ebag9* (sense, 5′-GCAACAGTGTTCTCGTTCCT-3′; antisense, 5′-TGGGCAAAGTTATTTGATC TCC-3′), *Cd8* (sense, 5′-GCTACCACAGGAGCCGAAAG-3′; antisense, 5′-TGG GCTTGCCTTCCTGTCT-3′), *Il10r* (sense, 5′-GAGCCCGTCTGTGAGCAAAC-3′; antisense, 5′-GATGGCCACGACGATCCA-3′), *Ifng* (sense, 5′-CCTTCTTCAGCAA CAGCAAGGCGAA-3′; antisense, 5′-GCAACAGCTGGTGGACCACTCG-3′), *Gzma* (sense, 5′- TGACTGCTGCCCACTGTAACG-3′; antisense, 5′-CGGCATCT GGTTCCTGGTTTCACA-3′), *Gzmb* (sense, 5′-CCATCGTCCCTAGAGCTGAG-3′; antisense, 5′-TTGTGGAGAGGGCAAACTTC-3′) and *Cxcr3* (sense, 5′-TCGGAC TTTGCCTTTCTTCTG-3′; antisense, 5′-CTCTCGTTTTCCCCATAATCGT-3′). Mouse *Gapdh* was used as an internal control. The results are shown as mean values ± s.d. Statistical analysis was carried out using Student's *t*-test.

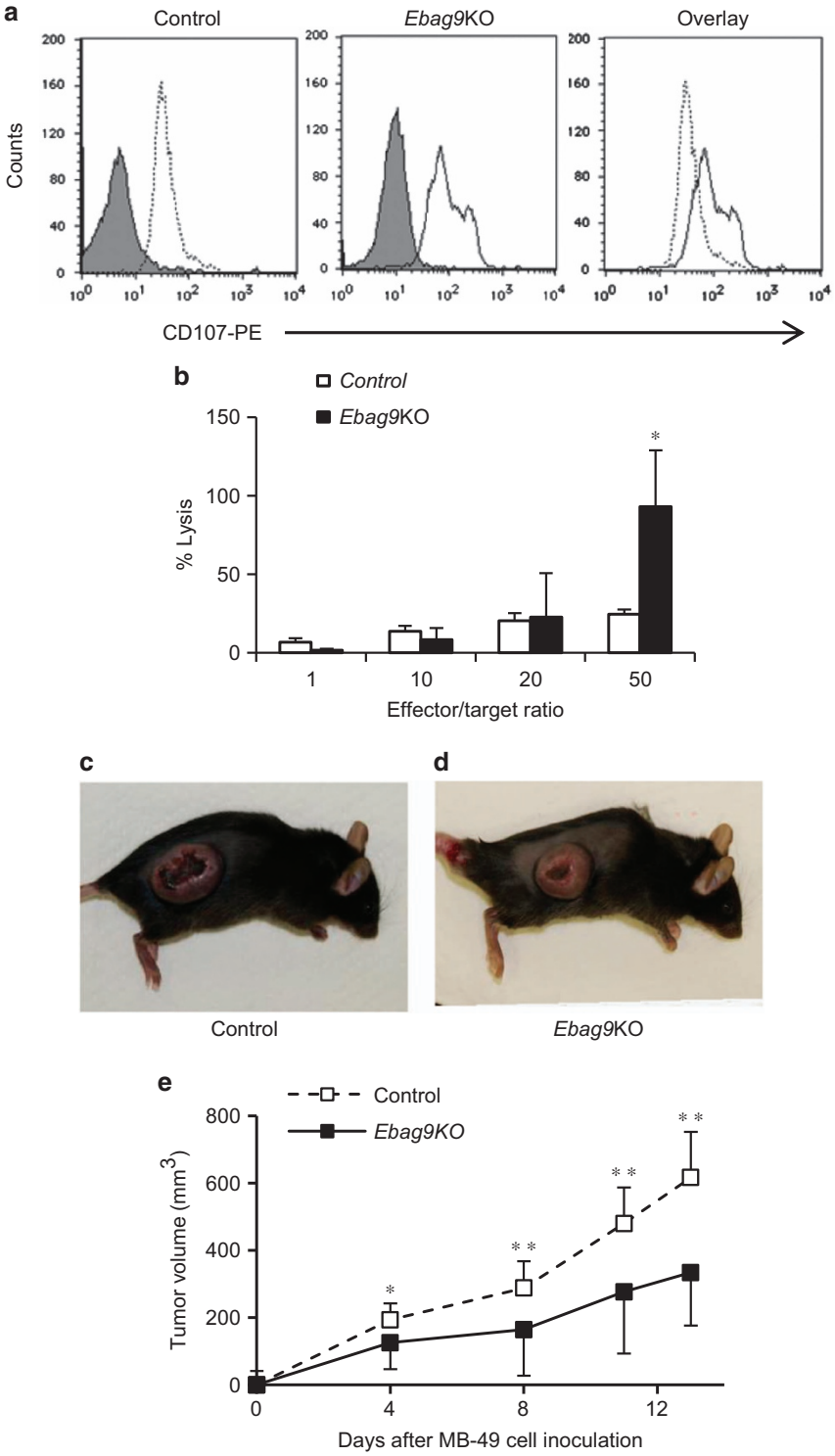

Figure 6. Promotion of degranulation and cytotoxic activity of $CD8^+$ T cells by EBAG9 knockout. (**a**) Flow cytometry-based degranulation assay of $CD8^+$ T cells from tumors in control (left) and *Ebag9*KO (middle) mice using phycoerythrin (PE)-conjugated anti-CD107 antibody. Overlap (right) of anti-CD107-PE fluorescence in *Ebag9*KO and control $CD8^+$ T cells illustrates the significant increase in degranulation due to *Ebag9* deletion. The peaks with grey shading represent cells stained with IgG2a–PE as a negative control. (**b**) Cytotoxicity assay of $CD8^+$ T cells from tumors in *Ebag9*KO and control mice. MB-49 cells (target) were incubated with $CD8^+$ T cells (effector) prepared from tumors generated in *Ebag9*KO and control mice at various effector/target ratios. The cytotoxic activity of $CD8^+$ T cells was monitored as the amount of lactate dehydrogenase in culture medium using the CytoTox 96 Non-Radioactive Cytotoxicity Assay. (**c** and **d**) $CD8^+$ T cells isolated from tumors generated in *Ebag9*KO mice exhibits antitumor activity. C57BL/6 mice were intravenously injected the $CD8^+$ T cells (2×10^6 cells per mouse) isolated from tumors generated in control (**c**) or *Ebag9*KO mice (**d**) and 2 days later, MB-49 cells were subcutaneously implanted into the recipient mice (5×10^5 cells per mouse). Tumor volumes were calculated once or twice a week. (**e**) Adaptive transfer of $CD8^+$ T cells from *Ebag9*KO mice significantly suppressed tumor growth by MB-49 cells implanted in C57BL/6 mice compared with those from control mice. The data shown are mean values ± s.d. $^*P < 0.05$, $^{**}P < 0.01$ by Student's *t*-test.

Western blot analysis

Cells were suspended in lysis buffer (20 mM HEPES, pH 7.9, 300 mM NaCl, 1 mM EDTA, 15% glycerol, 0.5% Nonidet P-40, 1 mM Na_3VO_4, 1 mM phenylmethylsulfonyl fluoride), rocked gently for 50 min at 4 °C, and centrifuged at 14 000 × *g* for 5 min at 4 °C. The supernatants were used as cell lysates. Cell lysates were resolved by sodium dodecyl sulfate polyacrylamide gel electrophoresis and electrophoretically transferred onto polyvinylidene difluoride membranes (EMD Millipore, Billerica, MA, USA). Membranes were probed with mouse anti-EBAG9 antibody or anti-β-actin monoclonal antibody.

In vivo tumor challenge

For subcutaneous implantation, MB-49 bladder cancer cells (5×10^5 cells per mouse) suspended in 50 µl of PBS were injected with 50 µl of Matrigel (Becton Dickinson, San Jose, CA, USA) into the flanks of *Ebag9*KO and control mice. Tumor volume was calculated three times a week. Mice were sacrificed 28 days after implantation and tumors were excised. The results are shown as mean values ± s.d. Statistical analysis was carried out using Student's *t*-test.

Immunohistochemistry

Immunohistochemical studies were done using the streptavidin–biotin amplification method with horseradish peroxidase detection. Paraffin sections of tumors were blocked in 0.3% $_{H2O2}$ (15 min) and incubated overnight with specific antibodies against CD3, CD4 or CD8 for bladder cancer tumors (1:200 dilution). Sections were incubated with antirabbit EnVision+ reagent (Dako) and counterstained with hematoxylin (Wako, Tokyo, Japan). The numbers of tumor-infiltrating lymphocytes positive for CD8, CD3 or CD4 expression were microscopically examined in the high-power field of view at a magnification of 400×. A spleen specimen from a control mouse was used as a positive control.

$CD8^+$ T-cell isolation

Mouse $CD8^+$ T cells were isolated from tumor tissue using a mouse CD8α-positive selection kit (STEMCELL Technologies, Vancouver, BC, Canada), according to the manufacturer's protocol. Isolated $CD8^+$ T cells were activated and expanded using a T-cell activation/expansion kit (Miltenyi Biotec, Bergisch Gladbach, Germany).

Degranulation assay

$CD8^+$ T cells isolated from tumors generated in *Ebag9*KO and control mice were washed with PBS and fixed with 70% ethanol. Cells were then washed and resuspended in FACS buffer (10 mM HEPES (pH 7.4), 140 mM NaCl, 2.5 mM $CaCl_2$) in the presence of anti-CD107a or IgG2a conjugated with PE. Degranulation was evaluated by flow cytometry and calculated as the percentage of cells that showed an increase in CD107a membrane fluorescence.

Cytotoxicity assay

MB-49 mouse bladder cancer cells were used as target cells. Target cells were incubated with effector $CD8^+$ T cells isolated from tumors generated in *Ebag9*KO and control mice at various effector/target ratios in a final volume of 100 µl for 8 h at 37 °C. Lactate dehydrogenase released from cells with damaged membranes was examined using the CytoTox 96 Non-Radioactive Cytotoxicity Assay (Promega, Madison, WI, USA) and absorbance was measured at 490 nm. Experiments were done in triplicate. The results are shown as mean values ± s.d. Statistical analysis was carried out using Student's *t*-test.

Adaptive $CD8^+$ T-cell transfer

Mouse $CD8^+$ T cells were isolated from tumor tissue in *Ebag9*KO and control mice using mouse CD8α-positive selection kit (STEMCELL Technologies). The $CD8^+$ T cells were intravenously injected into C57BL/6 mice (2×10^6 cells per mouse), after 2 days, the mice were inoculated with MB-49 cells (5×10^5 cells per mouse) that were suspended in 50 µl of PBS with 50 µl of Matrigel into the flank. Tumor volume was measured once or twice a week. The results are shown as mean values ± s.d. Statistical analysis was carried out using Student's *t*-test.

CONFLICT OF INTEREST

The authors declare no conflict of interest.

ACKNOWLEDGEMENTS

We thank Dr M Tanaka and Dr K Asano for their comments and suggestions. *Ayu1-Cre* mice were kindly provided by Dr K Yamamura. This work was supported in part by grants of the Cell Innovation Program, P-DIRECT and 'Support Project of Strategic Research Center in Private Universities' from the MEXT, Japan; by grants from the Ministry of Health, Labor and Welfare, the JSPS, the Advanced research for medical products Mining Program of the NIBIO and a grant from the Takeda Science Foundation.

REFERENCES

1 Watanabe T, Inoue S, Hiroi H, Orimo A, Kawashima H, Muramatsu M. Isolation of estrogen-responsive genes with a CpG island library. *Mol Cell Biol* 1998; **18**: 442–449.
2 Tsuchiya F, Ikeda K, Tsutsumi O, Hiroi H, Momoeda M, Taketani Y *et al.* Molecular cloning and characterization of mouse EBAG9, homolog of a human cancer associated surface antigen: expression and regulation by estrogen. *Biochem Biophys Res Commun* 2001; **284**: 2–10.
3 Suzuki T, Inoue S, Kawabata W, Akahira J, Moriya T, Tsuchiya F *et al.* EBAG9/RCAS1 in human breast carcinoma: a possible factor in endocrine-immune interactions. *Br J Cancer* 2001; **85**: 1731–1737.
4 Akahira JI, Aoki M, Suzuki T, Moriya T, Niikura H, Ito K *et al.* Expression of EBAG9/RCAS1 is associated with advanced disease in human epithelial ovarian cancer. *Br J Cancer* 2004; **90**: 2197–2202.
5 Takahashi S, Urano T, Tsuchiya F, Fujimura T, Kitamura T, Ouchi Y *et al.* EBAG9/RCAS1 expression and its prognostic significance in prostatic cancer. *Int J Cancer* 2003; **106**: 310–315.
6 Aoki T, Inoue S, Imamura H, Fukushima J, Takahashi S, Urano T *et al.* EBAG9/RCAS1 expression in hepatocellular carcinoma: correlation with tumour dedifferentiation and proliferation. *Eur J Cancer* 2003; **39**: 1552–1561.
7 Ogushi T, Takahashi S, Takeuchi T, Urano T, Horie-Inoue K, Kumagai J *et al.* Estrogen receptor-binding fragment-associated antigen 9 is a tumor-promoting and prognostic factor for renal cell carcinoma. *Cancer Res* 2005; **65**: 3700–3706.
8 Kumagai J, Urano T, Ogushi T, Takahashi S, Horie-Inoue K, Fujimura T *et al.* EBAG9 is a tumor-promoting and prognostic factor for bladder cancer. *Int J Cancer* 2009; **124**: 799–805.
9 Ijichi N, Shigekawa T, Ikeda K, Miyazaki T, Horie-Inoue K, Shimizu C *et al.* Association of positive EBAG9 immunoreactivity with unfavorable prognosis in breast cancer patients treated with tamoxifen. *Clin Breast Cancer* 2013; **13**: 465–470.
10 Engelsberg A, Hermosilla R, Karsten U, Schulein R, Dorken B, Rehm A. The Golgi protein RCAS1 controls cell surface expression of tumor-associated O-linked glycan antigens. *J Biol Chem* 2003; **278**: 22998–23007.
11 Julien S, Adriaenssens E, Ottenberg K, Furlan A, Courtand G, Vercoutter-Edouart AS *et al.* ST6GalNAc I expression in MDA-MB-231 breast cancer cells greatly modifies their O-glycosylation pattern and enhances their tumourigenicity. *Glycobiology* 2006; **16**: 54–64.
12 De Matteis MA, Luini A. Exiting the Golgi complex. *Nat Rev Mol Cell Biol* 2008; **9**: 273–284.
13 Rüder C, Höpken UE, Wolf J, Mittrücker HW, Engels B, Erdmann B *et al.* The tumor-associated antigen EBAG9 negatively regulates the cytolytic capacity of mouse CD8+ T cells. *J Clin Invest* 2009; **119**: 2184–2203.
14 Niwa H, Araki K, Kimura S, Taniguchi S, Wakasugi S, Yamamura K. An efficient gene-trap method using poly A trap vectors and characterization of gene-trap events. *J Biochem* 1993; **113**: 343–349.
15 Summerhayes IC, Franks LM. Effects of donor age on neoplastic transformation of adult mouse bladder epithelium in vitro. *J Natl Cancer Inst* 1979; **62**: 1017–1023.
16 Shankaran V, Ikeda H, Bruce AT, White JM, Swanson PE, Old LJ *et al.* IFNgamma and lymphocytes prevent primary tumour development and shape tumour immunogenicity. *Nature* 2001; **410**: 1107–1111.
17 Berman RM, Suzuki T, Tahara H, Robbins PD, Narula SK, Lotze MT. Systemic administration of cellular IL-10 induces an effective, specific, and long-lived immune response against established tumors in mice. *J Immunol* 1996; **157**: 231–238.
18 Zheng LM, Ojcius DM, Garaud F, Roth C, Maxwell E, Li Z *et al.* Interleukin-10 inhibits tumor metastasis through an systemic administration of cellular IL-10 induces an effective, specific, and long-lived immune response against established tumors in mice NK cell-dependent mechanism. *J Exp Med* 1996; **184**: 579–584.
19 Mumm JB, Emmerich J, Zhang X, Chan I, Wu L, Mauze S *et al.* IL-10 elicits IFNγ-dependent tumor immune surveillance. *Cancer Cell* 2011; **20**: 781–796.

20 Groux H, Bigler M, de Vries JE, Roncarolo MG. Inhibitory and stimulatory effects of IL-10 on human CD8+ T cells. *J Immunol* 1998; **160**: 3188–3193.
21 Santin AD, Hermonat PL, Ravaggi A, Bellone S, Pecorelli S, Roman JJ *et al.* Interleukin-10 increases Th1 cytokine production and cytotoxic potential in human papillomavirus-specific CD8(+) cytotoxic T lymphocytes. *J Virol* 2000; **74**: 4729–4737.
22 Jinquan T, Larsen CG, Gesser B, Matsushima K, Thestrup-Pedersen K. Human IL-10 is a chemoattractant for CD8+ T lymphocytes and an inhibitor of IL-8-induced CD4+ T lymphocyte migration. *J Immunol* 1993; **151**: 4545–4551.
23 Chen WF, Zlotnik A. IL-10: a novel cytotoxic T cell differentiation factor. *J Immunol* 1991; **147**: 528–534.
24 Halak BK, Maguire HC Jr, Lattime EC. Tumor-induced interleukin-10 inhibits type 1 immune responses directed at a tumor antigen as well as a non-tumor antigen present at the tumor site. *Cancer Res* 1999; **59**: 911–917.
25 Gérard CM, Bruyns C, Delvaux A, Baudson N, Dargent JL, Goldman M *et al.* Loss of tumorigenicity and increased immunogenicity induced by interleukin-10 gene transfer in B16 melanoma cells. *Hum Gene Ther* 1996; **7**: 23–31.
26 Emmerich J, Mumm JB, Chan IH, LaFace D, Truong H, McClanahan T *et al.* IL-10 directly activates and expands tumor-resident CD8(+) T cells without de novo infiltration from secondary lymphoid organs. *Cancer Res* 2012; **72**: 3570–3581.
27 Loetscher M, Gerber B, Loetscher P, Jones SA, Piali L, Clark-Lewis I *et al.* Chemokine receptor specific for IP10 and mig: structure, function, and expression in activated T-lymphocytes. *J Exp Med* 1996; **184**: 963–969.
28 Kundu N, Beaty TL, Jackson MJ, Fulton AM. Antimetastatic and antitumor activities of interleukin 10 in a murine model of breast cancer. *J Natl Cancer Inst* 1996; **88**: 536–541.
29 Loetscher M, Loetscher P, Brass N, Meese E, Moser B. Lymphocyte-specific chemokine receptor CXCR3: regulation, chemokine binding and gene localization. *Eur J Immunol* 1998; **28**: 3696–3705.
30 Cole KE, Strick CA, Paradis TJ, Ogborne KT, Loetscher M, Gladue RP *et al.* Interferon-inducible T cell alpha chemoattractant (I-TAC): a novel non-ELR CXC chemokine with potent activity on activated T cells through selective high affinity binding to CXCR3. *J Exp Med* 1998; **187**: 2009–2021.
31 Lu B, Humbles A, Bota D, Gerard C, Moser B, Soler D *et al.* Structure and function of the murine chemokine receptor CXCR3. *Eur J Immunol* 1999; **29**: 3804–3812.
32 Reckamp KL, Figlin RA, Moldawer N, Pantuck AJ, Belldegrun AS, Burdick MD *et al.* Expression of CXCR3 on mononuclear cells and CXCR3 ligands in patients with metastatic renal cell carcinoma in response to systemic IL-2 therapy. *J Immunother* 2007; **30**: 417–424.
33 Zipin-Roitman A, Meshel T, Sagi-Assif O, Shalmon B, Avivi C, Pfeffer RM *et al.* CXCL10 promotes invasion-related properties in human colorectal carcinoma cells. *Cancer Res* 2007; **67**: 3396–3405.
34 Harlin H, Meng Y, Peterson AC, Zha Y, Tretiakova M, Slingluff C *et al.* Chemokine expression in melanoma metastases associated with CD8+ T-cell recruitment. *Cancer Res* 2009; **69**: 3077–3085.
35 Jones D, Benjamin RJ, Shahsafaei A, Dorfman DM. The chemokine receptor CXCR3 is expressed in a subset of B-cell lymphomas and is a marker of B-cell chronic lymphocytic leukemia. *Blood* 2000; **95**: 627–632.
36 Narvaiza I, Mazzolini G, Barajas M, Duarte M, Zaratiegui M, Qian C *et al.* Intratumoral coinjection of two adenoviruses, one encoding the chemokine IFN-gamma-inducible protein-10 and another encoding IL-12, results in marked antitumoral synergy. *J Immunol* 2000; **164**: 3112–3122.
37 Pan J, Burdick MD, Belperio JA, Xue YY, Gerard C, Sharma S *et al.* CXCR3/CXCR3 ligand biological axis impairs RENCA tumor growth by a mechanism of immunoangiostasis. *J Immunol* 2006; **176**: 1456–1464.
38 Peters PJ, Borst J, Oorschot V, Fukuda M, Krahenbuhl O, Tschopp J *et al.* Cytotoxic T lymphocyte granules are secretory lysosomes, containing both perforin and granzymes. *J Exp Med* 1991; **173**: 1099–1109.
39 Minegishi N, Ohta J, Yamagiwa H, Suzuki N, Kawauchi S, Zhou Y *et al.* The mouse GATA-2 gene is expressed in the para-aortic splanchnopleura and aorta-gonads and mesonephros region. *Blood* 1999; **93**: 4196–4207.
40 Suwabe N, Takahashi S, Nakano T, Yamamoto M. GATA-1 regulates growth and differentiation of definitive erythroid lineage cells during in vitro ES cell differentiation. *Blood* 1998; **92**: 4108–4118.